



Original Research

Identification of leucine-rich repeat-containing protein 59 (LRRC59) located in the endoplasmic reticulum as a novel prognostic factor for urothelial carcinoma

Lu Pei^{a,1}, Qingfeng Zhu^{b,1}, Xiaoping Zhuang^c, Honglian Ruan^d, Zhiguang Zhao^e,
Haide Qin^{a,f,**}, Qiongqiong Lin^{e,*}

^a Guangdong Provincial Key Laboratory of Malignant Tumor Epigenetics and Gene Regulation, Sun Yat-sen Memorial Hospital, Sun Yat-sen University, Guangzhou 510120, China

^b Department of Urology, Lishui Municipal Central Hospital, Lishui, China

^c Department of Pathology, Wenzhou Hospital of Integrated Traditional Chinese and Western Medicine, Wenzhou, China

^d School of Public Health, Guangzhou Medical University, Xinzao Town, Panyu District, Guangzhou, Guangdong 511436, China

^e Department of Pathology, The Second Affiliated Hospital and Yuying Children's Hospital of Wenzhou Medical University, 109 Xueyuan Western Road, Wenzhou 325027, China

^f Department of Urology, Sun Yat-sen Memorial Hospital, Sun Yat-sen University, Guangzhou, China

ARTICLE INFO

Keywords:

Urothelial carcinoma
Leucine-rich repeat-containing protein
Prognosis
Endoplasmic reticulum stress
Ubiquitination

ABSTRACT

Background: Urothelial carcinoma (UC) is one of the most common cancers worldwide. The biological heterogeneity of UCs causes considerable difficulties in predicting treatment outcomes and usually leads to clinical mismanagement. The identification of more sensitive and efficient predictive biomarkers is important in the diagnosis and classification of UCs. Herein, we report leucine-rich repeat-containing protein 59 (LRRC59) located in the endoplasmic reticulum as a novel predictive factor and potential therapeutic target for UCs.

Methods: Using whole-slide image analysis in our cohort of 107 UC samples, we performed immunohistochemistry to evaluate the prognostic value of LRRC59 expression in UCs. *In vitro* experiments using RNAi were conducted to explore the role of LRRC59 in promoting UC cell proliferation and migration.

Results: A significant correlation between LRRC59 and unfavorable prognosis of UCs in our cohort was demonstrated. Subsequent clinical analysis also revealed that elevated expression levels of LRRC59 were significantly associated with higher pathological grades and advanced stages of UC. Subsequently, knockdown of LRRC59 in UM-UC-3 and T24 cells using small interfering RNA significantly inhibited cell proliferation and migration, resulting in cell cycle arrest at the G1 phase. Conversely, the overexpression of LRRC59 in UC cells enhanced cell proliferation and migration. An integrated bioinformatics analysis revealed a significant functional network of LRRC59 involving protein misfolding, ER stress, and ubiquitination. Finally, *in vitro* experiments demonstrated that LRRC59 modulates ER stress signaling.

Conclusions: LRRC59 expression was significantly correlated with UC prognosis. LRRC59 might not only serve as a novel prognostic biomarker for risk stratification of patients with UC but also exhibit as a potential therapeutic target in UC that warrants further investigation.

Abbreviations: urothelial carcinoma, (UC); non-muscle invasive bladder cancer, (NMIBC); Muscle invasive bladder cancer, (MIBC); post-translational modifications, (PTMs); endoplasmic reticulum, (ER); endoplasmic reticulum stress, (ERS); unfolded protein response, (UPR); extracellular vesicles, (EVs); LRRC59, (leucine-rich repeat-containing protein 59); whole slide image, (WSI); Immunohistochemistry, (IHC); formalin-fixed paraffin-embedded, (FFPE); gene expression omnibus, (GEO); the cancer genome atlas, (TCGA); human protein atlas, (HPA); small interfering RNA, (siRNA); tunicamycin, (TM); fibroblast growth factor 1, (FGF1); ubiquitin proteasomal system pathway, (UPS); stress granules, (SGs).

* Corresponding author at: Department of Pathology, the Second Affiliated Hospital and Yuying Children's Hospital of Wenzhou Medical University, 109 Xueyuan Western Road, Wenzhou, China.

** Corresponding author at: Guangdong Provincial Key Laboratory of Malignant Tumor Epigenetics and Gene Regulation, Sun Yat-sen Memorial Hospital, Sun Yat-sen University, Guangzhou 510120, China.

E-mail addresses: qinhd3@mail.sysu.edu.cn (H. Qin), linqiongqiong@wmu.edu.cn (Q. Lin).

¹ These authors contributed equally to this work.

<https://doi.org/10.1016/j.tranon.2022.101474>

Received 27 April 2022; Received in revised form 14 June 2022; Accepted 27 June 2022

1936-5233/© 2022 Published by Elsevier Inc. This is an open access article under the CC BY-NC-ND license (<http://creativecommons.org/licenses/by-nc-nd/4.0/>).

Introduction

Urothelial carcinoma (UC) is one of the most common cancers worldwide [1]. Frequent recurrence rates and high risk of metastasis in UC pose significant challenges for the treatment of UC. In the treatment of muscle-invasive bladder cancer (MIBC), platinum-based neoadjuvant chemotherapy followed by radical cystectomy is the current standard of care [2]. However, approximately 70% of patients have tumor metastasis, and the 5-year survival remains extremely poor [3]. As a result, the identification of more efficient and accurate molecular biomarkers is important in the risk stratification of patients with UC for individualized management.

Previous studies have established that clinical factors, such as lymph nodes (LN) status and T stage, are important factors that affect the prognosis of patients with UC. The 5-year overall survival rate of LN-positive patients is <30% [4]. Although several studies have indicated that predictive models incorporating genetic and clinical factors are useful in predicting the prognosis of UC, few studies have validated the utility of predictive models for the improvement of clinical decision-making [5,6]. Moreover, owing to the striking molecular heterogeneity, patients with UC with the same grade and stage might present distinct outcomes. For example, patients at the early stage, such as Tis or basal-squamous differentiation, show aggressive phenotypes and resistance to treatment [7,8]. Currently, no reliable tools are available to distinguish tumors that have the potential to progress. Therefore, there is a need to identify novel biomarkers for improving the diagnostic accuracy of UC.

Emerging studies have shown that post-translational modifications (PTMs), which mainly occur in the endoplasmic reticulum (ER), are important for cancer development and progression [9,10]. The ER is an essential organelle for protein folding and quality control. Protein misfolding in tumor cells results in ER stress (ERS), triggers unfolded protein response (UPR), and guides unfolded proteins into the cytoplasm for ubiquitination and destruction via the proteasome [11]. Moreover, induction of UPR and ERS leads to extracellular vesicle formation and promotes cell proliferation, tumor progression, and recurrence [12]. However, the role of ERS/UPR signaling in the progression of UCs remains unclear.

The present study, using a data-driven approach to identify the pathogenic genes in UCs, showed a strong correlation network associated with poor prognosis of UCs, which involved multiple ER proteins, including leucine-rich repeat-containing protein 59 (LRRC59). To elucidate the roles of LRRC59-mediated PTM in UC, using whole-slide image (WSI) and bioinformatics analyses, we validated that LRRC59 is a novel biomarker with prognostic value for risk stratification and robust prediction of overall survival for patients with UC. Functional studies further showed that LRRC59 plays an important role in the regulation of tumor cell proliferation and migration. Thus, LRRC59 may also serve as a potential therapeutic target for UCs.

Materials and methods

Patient data

A total of 107 patients diagnosed with urothelial carcinoma between January 2014 and March 2020 were included as study subjects. All study subjects were from the Second Affiliated Hospital and Yuying Children's Hospital of Wenzhou Medical University (WMU). The pathologic diagnosis was based on the eighth edition of the American Joint Committee on Cancer [13]. Written informed consent was obtained from all patients. This study was performed in accordance with the Declaration of Helsinki (revised in 2013). All experimental protocols were approved by the Ethics Committee of the Second Affiliated Hospital and Yuying Children's Hospital of WMU (2021-K-101-01).

IHC analysis

To elucidate the expression of LRRC59 in UC, formalin-fixed paraffin-embedded UC samples were cut into 3 μm -thick serial sections. Immunostaining of the sections was conducted on the Ventana BenchMark Ultra platform (Roche Diagnostics, Tucson). Briefly, slides were incubated for 8 min in EZPrep for deparaffinization and antigen retrieval. Sections were incubated in Cell Conditioner 1 (prediluted; pH 8.0) for 30 min at 37 °C and then for 8 min at 37 °C in UV inhibitor. Anti-LRRC59 antibody was added at a 1:200 dilution for 32 min at 37 °C. UV HRP UNIV MULT (secondary antibody) was added and incubated for 8 min. Then, the specimen was counterstained with hematoxylin II and bluing reagent (Ventana) and coverslipped. Rabbit polyclonal antibodies against LRRC59 (aa 84-307) were purchased from Abcam (#ab184143). Lung adenocarcinoma and colorectal carcinoma were used as positive controls, according to the Human Protein Atlas (HPA) database and previous studies [14]. The primary antibody was used as a negative control.

IHC evaluation

IHC was conducted to analyze the expression of LRRC59, which showed a granular cytoplasmic staining pattern. Immunostaining was evaluated based on the staining intensity of positive cells [14,15]. The color intensity of the cytoplasm was scored as follows: 0, no staining; 1, weak staining; 2, medium staining; and 3, strong staining. A score of 0 indicated a negative result. A score of 1–3 indicated a positive result. IHC staining was evaluated by two independent pathologists in a blinded manner.

Using the NanoZoomer XR Digital Pathology microscope (Hamamatsu Photonics KK, Hamamatsu), all slides were scanned as WSIs at a magnification of 40 \times .

WSI analysis

The QuPath software [16] (version 0.2.1) was used to perform automated quantification of H-scores from whole-slide immunohistochemistry images. The original IHC slides were scanned and subjected to subsequent analysis. For each IHC slide, the estimate stain vectors command was used to facilitate stain separation. In the QuPath software, five representative regions of interest (ROIs) were manually selected by a pathologist using the Squared Tool (250 μm \times 250 μm). Then, an in-house Groovy Script was created for WSI analysis to automatically calculate the mean H-scores for the ROIs for each slide.

Data source and bioinformatics analysis

In-house R scripts were used for data processing, analysis, and visualization. Gene expression data and corresponding clinical information were obtained from publicly available databases, including Gene Expression Omnibus (GEO) datasets (<http://www.ncbi.nlm.nih.gov/gds/>), The Cancer Genome Atlas (TCGA, <https://tcga-data.nci.nih.gov/tcga/>), cBioPortal (<https://www.cbioportal.org/>), and the HPA database (<http://www.proteinatlas.org/>). Enrichment analyses were conducted using the WebGestalt software (WEB-based Gene Set Analysis Toolkit, <http://www.webgestalt.org/>). Producer price index (PPI) analysis was conducted using STRING (<https://string-db.org/>). The SEEK platform was used for gene co-expression analysis in bladder cancer microarray datasets GSE31684, GSE3167, and GSE32548 (<http://seek.princeton.edu/seek/>).

Cell culture

The human urothelial carcinoma cell lines T24 and UM-UC-3 cell lines used in this study were purchased from the American Type Culture Collection (ATCC, Manassas, VA, USA). T24 cells were cultured in RPMI-

1640 complete medium (Gibco, Gaithersburg, MD, USA), whereas UM-UC-3 cells were cultured in DMEM complete medium (Gibco, Gaithersburg, MD, USA). The complete medium was supplemented with 10% fetal bovine serum (FBS; Sigma-Aldrich, Darmstadt, Germany) and 1% penicillin/streptomycin (Gibco, Gaithersburg, MD, USA). All cell lines were carefully cultured in a humidified atmosphere with 5% CO₂ at 37 °C. To induce ER stress, tunicamycin (TM, 2 µg/mL, MedChemExpress, USA) dissolved in sterile dimethyl sulfoxide (DMSO) was added to the culture medium in the presence or absence of siLRRC59s.

RNA extraction and quantitative real-time (qRT)-PCR

Total RNA was extracted from the cell lines using TRIzol reagent (Invitrogen, Shanghai, China). cDNA was synthesized using the PrimeScript™ RT Reagent Kit (Takara, Shiga, Japan). qRT-PCR was performed on cDNA samples using TB Green Premix Ex TaqII (Takara Bio, Shiga, Japan). Fluorescent signals were detected by the Quantstudio Dx system (Applied Biosystems, Singapore) according to the manufacturer's instructions. The mRNA levels of LRRC59, HYOU1, XBP1, E2F1 were normalized to GAPDH using the 2^{-ΔΔCT} method. The primer sequences were as follows: LRRC59, 5'-GAAGAAGCGTGAGGCTAAGCA-3'(forward), 5'-TTAGATTTCCGGGCGCTGATTTG-3'(reverse); HYOU1, 5'-GAGGAGCGGAGTCTGTGG-3'(forward), 5'-GCACTCCAGTTTGACAA TGG-3'(reverse); XBP1, 5'-CCCTCCAGAACATCTCCCAT-3'(forward), 5'-ACATGACTGGGTCCAAGTTGT-3'(reverse); E2F1, 5'-CATCCAG-GAGGTCACCTTG-3'(forward), 5'-GACAACAGCGTTCTTGCTC-3'(reverse); GAPDH, 5'-ACAACCTTGGTATCGTGAAGG-3'(forward), 5'-GCC ATCAGCCACAGTTTC-3'(reverse).

RNA interference

Small interfering RNA (siRNA) duplexes targeting LRRC59 were synthesized by GenePharma (Shanghai, China). Nonspecific siRNA sequences were used as negative control. siRNAs were transfected into cells using Lipofectamine RNAiMax (Life Technologies, Waltham, MA, USA) according to the manufacturer's instructions. The sequences of the siRNAs were as follows: silencing control (siCtrl), UUCUCCGAACGU-GUCACGUTT; siLRRC59#1, GUGACUGCUUGGAUGAGAATT; and siLRRC59#2, GGAGUAUGAUGCCCUCAAATT.

Plasmid construction and transfection

The coding sequence of LRRC59 was cloned into a pcDNA3.1(+) vector (IGE Biotechnology, Guangzhou, China) to construct LRRC59 overexpression plasmid. Plasmid vectors were transfected into urothelial carcinoma cells cultured in six-well plates using X-tremeGENE (Sigma-Aldrich, St. Louis, MO, USA), following the manufacturer's protocol. Cells were harvested for qRT-PCR analysis 48 h after transfection.

CCK-8 assay

Cell viability was evaluated using the CCK8 Cell Counting Kit (Dojindo Laboratories, Kumamoto, Japan). T24 and UM-UC-3 cells transfected with siLRRC59s or pcDNA3.1(+)-LRRC59 were plated and cultured in 96-well plates with 1.0 × 10³ cells/well and incubated at the temperature of 37 °C for 6 days. Detection was performed at the same time points each day. The optical density (OD) values were measured at 450 nm using a microplate reader (Tecan, Switzerland). The experiments were performed in triplicate for each cell line.

Colony formation assay

Cells were placed in six-well plates (1 × 10³ cells/well) and maintained in media containing 10% FBS for 14 days. The colonies were fixed with 4% paraformaldehyde (Servicebio, Wuhan, China) and stained

with 0.1% crystal violet (Sigma-Aldrich, Darmstadt, Germany). Colonies were imaged using vSpot Spectrum (AID, Germany). All assays were performed three times for each cell line.

Cell cycle analysis

The cancer cells were harvested at 48 h after the transfection of siLRRC59s, then washed with ice-cold PBS, and fixed in 75% ice-cold ethanol at 4 °C. RNaseA (Takara, Shiga, Japan) was added into the flow tubes, followed by a water bath at 37 °C for 30 min. For staining, the cells were incubated in propidium iodide (PI, Life Technologies) solution for 10 min in dark. Flow cytometry analysis of the cell cycle for the treated cells was performed by CytoFLEX (Beckman, USA). The experiments were performed in triplicate.

Transwell assay

The migration ability of UC cells was estimated by Transwell assay. Transwell chambers with a pore size of 8.0 µm (Millipore, Darmstadt, Germany) were used in this assay. Cells were suspended in 200 µL serum-free medium evenly and plated in Transwell chambers. 600 µL medium supplemented with 10% FBS was added to the twenty-four-well plates as a chemoattractant. After incubation for 20 h (UM-UC-3 cells) or 8 h (T24 cells), the migrated cells at the bottom of the chambers were fixed in 4% paraformaldehyde and then stained with 0.1% crystal violet solution for 15 min. Then, the cells in the lower chamber were counted. All experiments were performed in triplicate.

Statistical analysis

Survival analysis was conducted using statistical R language (<https://www.r-project.org/>). The analytic packages include *survival*, *ggsurv*, and *rbsurv* for robust likelihood-based survival modeling. For visualization and the log-rank test, GraphPad Prism version 8 was used to generate plots. We used a p-value < 0.05 as a significant level to interpret the results. Hypoxia score correlation analysis was performed using the TCGA/cBioPortal (<https://www.cbioportal.org/>). Comparisons between the two groups were performed using Student's *t*-test, and Mann-Whitney U test. The data are indicated as standard error of the mean (SEM), and a p-value < 0.05 was considered statistically significant. Gene-gene correlations and predictive model building were performed using in-house R scripts based on the package *caret*. Fisher's exact test was used for the association test between gene expression levels and clinical variables. Univariate and multivariate Cox regression analyses were performed using R script.

Results

Screening of the pathogenic biomarkers for the prediction of prognosis of UC

To identify the oncogenic genes for predicting poor outcome of UCs, we screened the upregulated genes with potential prognostic prediction capabilities in UCs. As shown in Fig. 1, we first identified upregulated genes in UC samples using the publicly available TCGA-BLCA dataset. Then, the unfavorable prognostic genes in bladder cancer characterized in the HPA database were obtained and intersected with the upregulated genes. The resulting 14 highly confident oncogenic genes were inspected and finally generated for subsequent analyses (Fig. 1A). Univariate analysis of the oncogenic prognostic genes identified LRRC59 at the top of the list (Supplementary Table S1).

To further characterize the highly confident oncogenic genes, we first explored their expression patterns in cells. We found that LRRC59, SCD, DHCR7, and RPN2 were located in the cellular ER in the HPA dataset, suggesting the important role of abnormal ER function in UC progression. Then, we conducted co-expression analysis to identify the

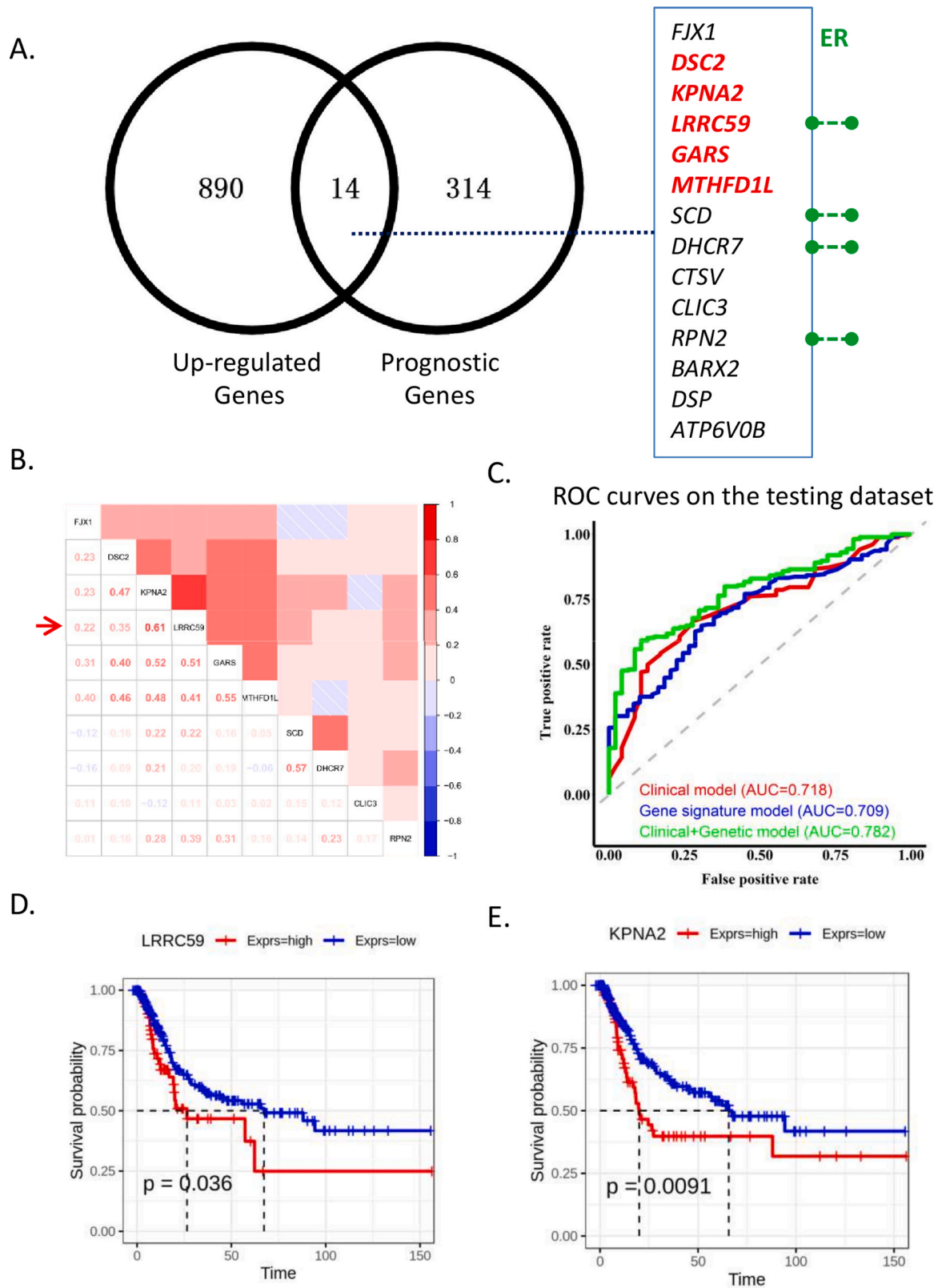


Fig. 1. Screening of unfavorable prognostic genes in UCs. (A) Venn diagram demonstrated the upregulated unfavorable prognostic genes in bladder cancer. (B) Correlation matrix of the upregulated unfavorable prognostic genes. (C) ROC plots for the prediction of the prognosis of bladder cancer in the testing dataset in TCGA/BLCA. (D, E) Survival curves for the comparisons of the high and low expression levels for the LRRC59 and KPNA2 genes identified in UCs.

co-expression network associated with the pathogenesis of UC. A correlation heatmap showed that there was a significant co-expression network involving DSC2, KPNA2, LRRC59, GARS, and MTHFD1L (Fig. 1B).

Furthermore, we built a model using the training dataset (70% of the entire dataset) derived from the TCGA-BLCA dataset and tested the model using the testing dataset (30% of the entire dataset). We found that the identified genes performed well in the prediction of the prognosis of bladder cancer in testing dataset (the genomic model had AUC of 0.709 to predict 60-month survival) (Fig. 1C). Among these, LRRC59 and KPNA2 showed the strongest correlation in the expression levels. Higher expression levels of the two genes were significantly correlated with unfavorable prognosis in bladder cancer (log-rank p -value < 0.05) (Fig. 1D; 1E; Supplementary Fig. S1). Based on previous studies, the functions of KPNA2 on the nuclear membrane have been characterized in UCs [17], but the roles of LRRC59 remain to be determined.

LRRC59 serves as a novel prognostic biomarker in UCs

To characterize the functions and roles of LRRC59, we profiled protein expression using an IHC assay in UC samples. We found that LRRC59 was mainly localized in the cytoplasm of cancer cells. LRRC59 expression was not detected in the nuclei. The expression levels of

LRRC59 in tumor cells were strikingly upregulated compared with those in the adjacent normal urothelium (Fig. 2A). Interestingly, LRRC59 overexpression was primarily found in tumor cells but not in umbrella cells (Fig. 2B). The upregulation of LRRC59 in our results was consistent with those found in the TCGA and GSE3167 datasets (Supplementary Fig. S2).

To investigate whether LRRC59 can be regarded as a prognostic biomarker, we explored the effect of LRRC59 on the prognosis of patients with UC. From the survival analysis, we observed that the positive expression levels of LRRC59 were closely associated with worse survival of UCs compared with the negative expression of LRRC59, with a log-rank p -value of 0.045 in our cohort ($n = 107$) (Fig. 3A and B). Patients with higher tumor H-scores showed a significant correlation with poor survival (Fig. 3C). In multivariate Cox proportional hazards survival analysis, LRRC59 expression was shown to be an independent risk factor in the prediction of UCs (95%CI, 1.45–7.5, p -value = 0.004) (Fig. 4).

Thus far, LRRC59 has not been correlate with UCs in previous studies. In the current study, a strong association with worse outcomes indicated that LRRC59 might be considered as a predictive biomarker for the prognosis of UCs.

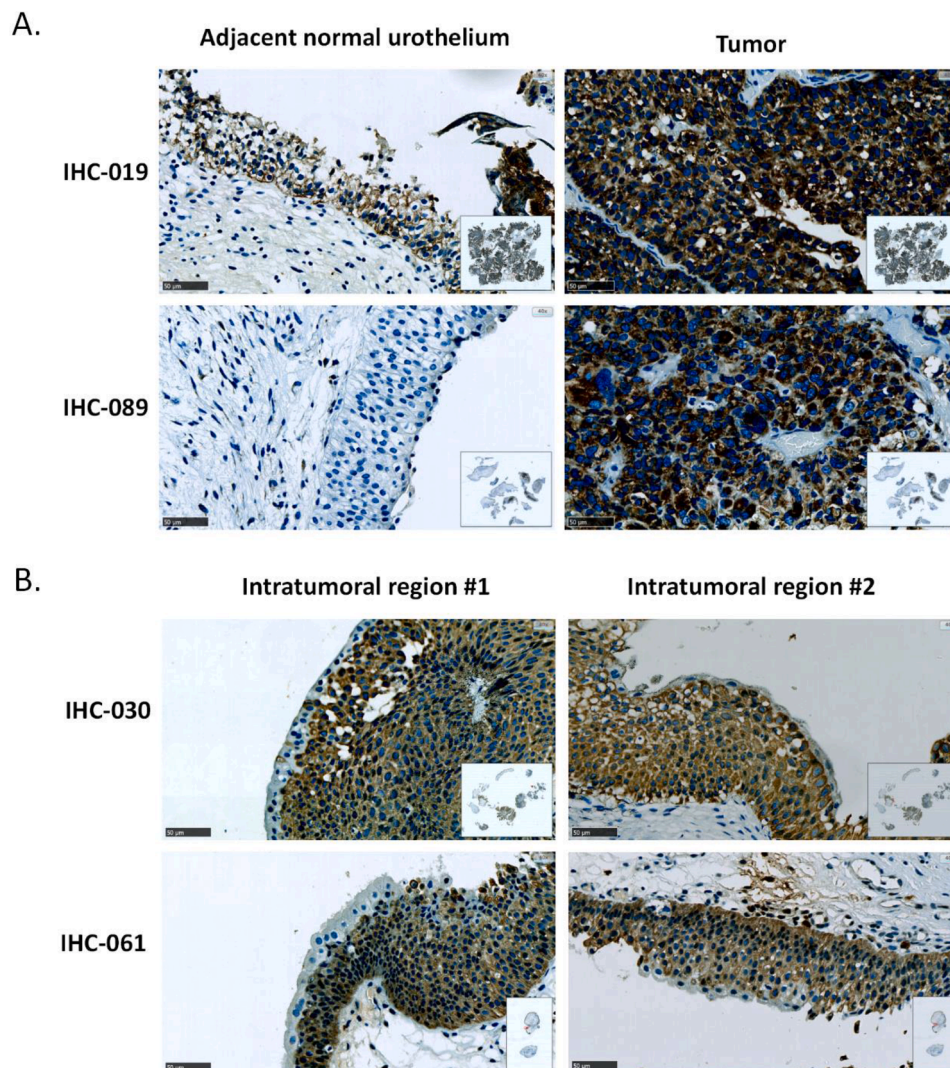


Fig. 2. Representative images of LRRC59 expression in UC samples. (A) The expression patterns of LRRC59 in the adjacent normal urothelium and tumor tissue within the same sample. Scale bar: 50 μm; magnification at 400 × . (B) LRRC59 was upregulated in tumor cells but not in umbrella cells.

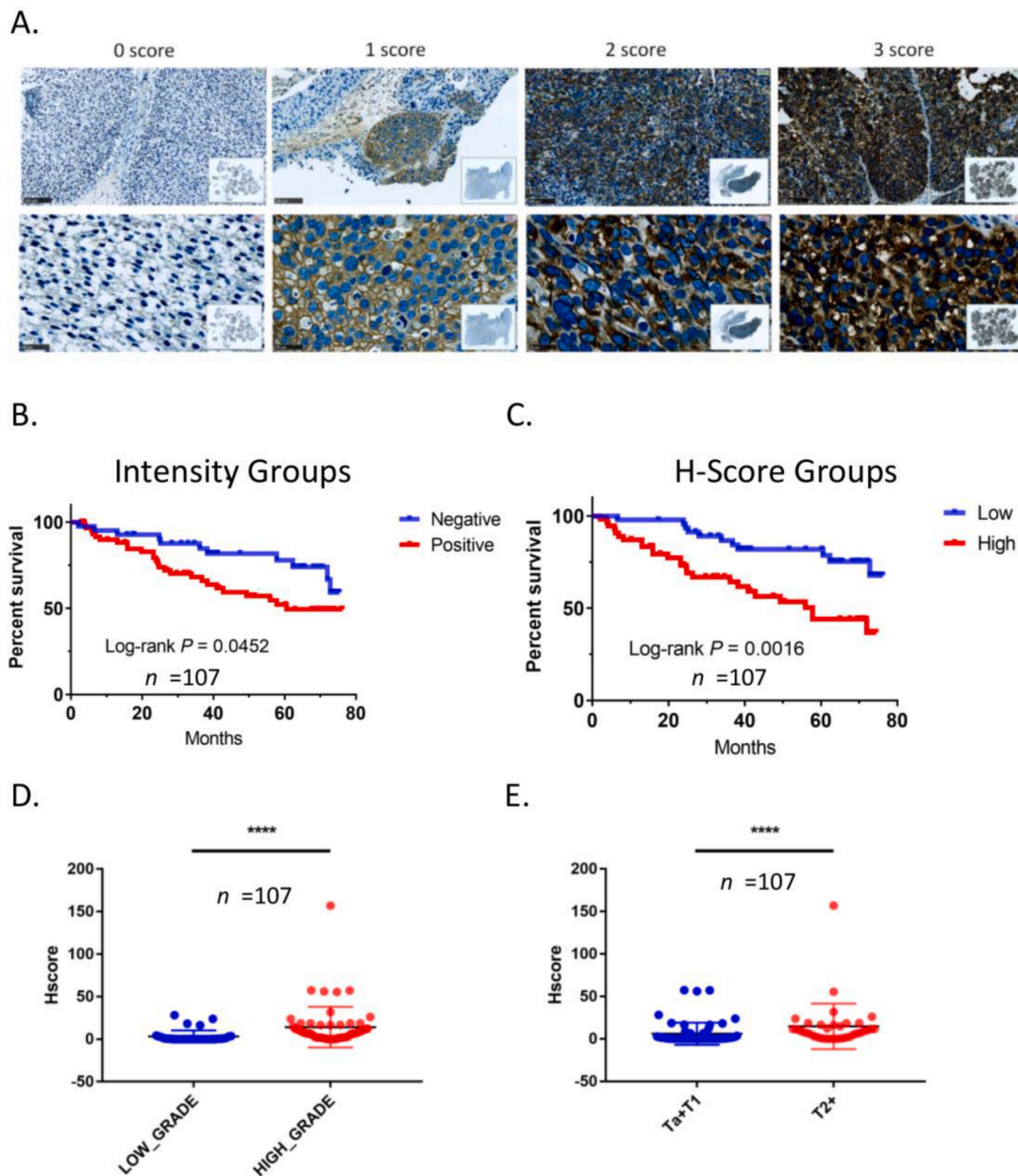


Fig. 3. Elevated expression levels of LRRRC59 were revealed as clinically relevant. (A) Representative images to indicate IHC staining intensities. Scale bar (top): 100 μ m; magnification at $200\times$. Scale bar (bottom): 25 μ m; magnification at $800\times$. (B) The elevated expression levels of LRRRC59 were significantly correlated with poorer survival of UCs in our cohort ($n = 107$). Scale bar: 50 μ m; magnification at $400\times$. (C) Higher H-score was associated with poorer median survival compared with low H-score from our cohort. (D) Based on H-score, significant differences were found between high-grade UCs and low-grade UCs. (E) Based on H-score, significant differences were found between NMIBC and MIBC. NMIBC, non-muscle-invasive bladder cancer; MIBC, muscle-invasive bladder cancer. **** $p < 0.0001$.

Upregulated level of LRRRC59 was significantly associated with higher tumor grades and advanced stages of UC

Next, to investigate the correlation between LRRRC59 gene expression and clinical factors, we analyzed the association between LRRRC59 gene expression levels and covars, tumor grades, and stages (Table 1). Of the 107 UC samples, 43% (46/107) had low-grade tumors and 57% (61/107) had high-grade tumors. The positive staining of LRRRC59 was observed in 64 cases, including 14 (21.8%) low-grade UC cases and 50 (78.2%) high-grade UC cases. Of the 61 high-grade UC cases, LRRRC59 expression was observed in 50 (82%). However, of the 46 low-grade UC cases, LRRRC59 expression was found in only 14 (30.5%). These results showed that the expression levels of LRRRC59 were elevated in high-grade tumors, which indicated that the enhancement of LRRRC59

expression might be highly linked to UC grades (Fig. 3D).

To further assess whether LRRRC59 is involved in UC progression, we analyzed the expression levels of LRRRC59 in both non-muscle-invasive bladder cancer (NMIBC) and MIBC. Our cohort of 107 cases consisted of 63 NMIBC and 36 MIBC cases. Of the 63 NMIBC cases, 50.8% (32/63) were positive for LRRRC59 expression. Among the 36 MIBC cases, positive staining for LRRRC59 was found in 83.4% (30/36) of the samples. LRRRC59 expression is increased in MIBC. Our findings suggest that LRRRC59 plays an important role in UC progression (Fig. 3E).

LRRRC59 promoted the proliferation and migration of UC cells

To explore the biological functions of LRRRC59 in UC cells, siLRRRC59s and pcDNA 3.1(+)-LRRRC59 were respectively transfected into T24 and

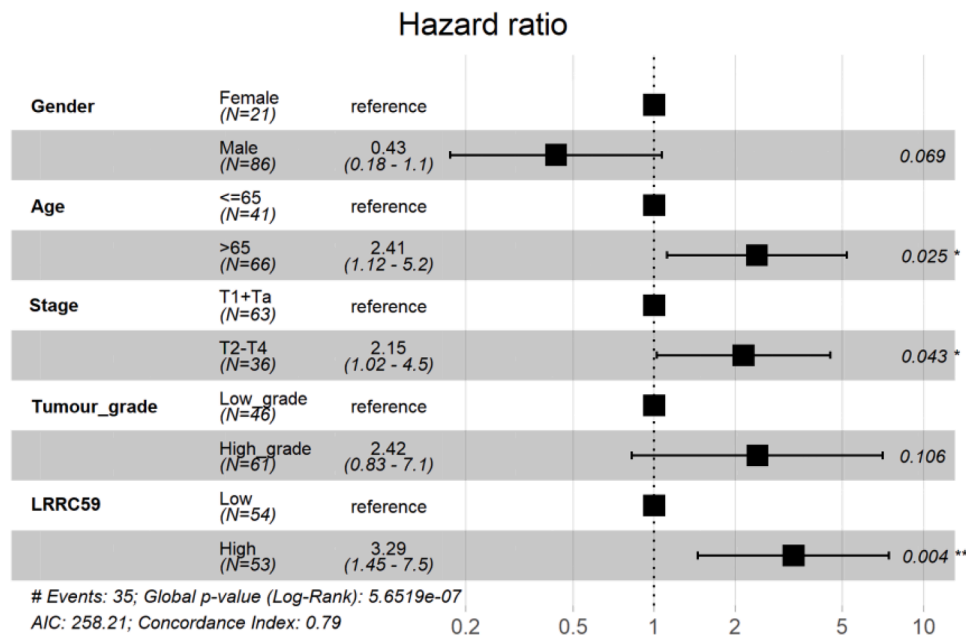


Fig. 4. Multivariate Cox proportional hazards survival analysis of LRRC59. * $p < 0.05$. ** $p < 0.01$.

Table 1

Association analysis of the expression levels of LRRC59 with the clinical-pathological variables of urothelial carcinoma patients.

Variables	LRRC59 (n, %)*		Total	OR(95%CI)	p-value
	Low	High			
Gender					
Female	10 (18.5)	11 (20.8)	21 (19.6)		
Male	44 (81.5)	42 (79.2)	86 (80.4)	0.87(0.33-2.27)	0.771
Age (years)					
≤65	23 (42.6)	18 (34.0)	41 (38.3)		
>65	31 (57.4)	35 (66.0)	66 (61.7)	1.44(0.66-3.19)	0.3593
Stage					
Ta-T1	41 (75.9)	22 (41.5)	63 (58.9)		
T2-T4	9 (16.7)	27 (50.9)	36 (33.6)	5.59(2.31-14.60)	0.000228
Missing	4 (7.4)	4 (7.5)	8 (7.5)		
Grade					
Low grade	37 (68.5)	9 (17.0)	46 (43.0)		
High grade	17 (31.5)	44 (83.0)	61 (57.0)	10.6(4.41-28.00)	4.53E-07

* Defined by the best cut-off value.

UM-UC-3 cells, resulting in the remarkable downregulation or upregulation of LRRC59 mRNA level (Fig. 5A and B). CCK-8 assays showed that the proliferation of UM-UC-3 and T24 cells in the siLRRC59s group was significantly impaired compared with the siCtrl group (Fig. 5C and D). In contrast, when LRRC59 was overexpressed, T24 and UM-UC-3 cells exhibited a higher cell viability rate than the controls (Fig. 5E and F). Consistently, colony-formation assays revealed that the size and number of colonies in both cell lines were dramatically inhibited by siLRRC59s compared to the siCtrl group (Fig. 5G and H), while cell lines with high expression of LRRC59 were markedly increased (Fig. 5I and J). Furthermore, Transwell assay showed that silencing of LRRC59 caused a significant reduction of the migrated UM-UC-3 and T24 cells (Fig. 5K and L). Conversely, we found that the overexpression of LRRC59 promoted UC cell migration (Fig. 5M and N). These data indicate that LRRC59 plays a vital role in cancer cell migration and tumor proliferation.

Knockdown of LRRC59 induced cell cycle arrest

To further determine whether LRRC59 silencing inhibited cell viability by affecting the tumor cell cycle progression, we performed flow cytometric analysis to examine cell cycle alterations in the UC cell lines. Consistently, UC cells were significantly increased in the G1 phase in both UM-UC-3 and T24 cells transfected with siLRRC59s compared with the siCtrl group (Fig. 6D–G), which suggests that cells with LRRC59 silencing were arrested at the G1 phase.

LRRC59 co-expression networks were correlated to PTMs at the ER

To investigate the potential upstream factors modulating LRRC59, we conducted bioinformatics analysis using the TCGA-BLCA dataset. We found that elevated expression levels of LRRC59 were significantly correlated with copy number amplifications of the genes and higher hypoxia scores (Supplementary Fig. S3) in the TCGA-BLCA cohort, suggesting that LRRC59 was regulated by copy number alternations and might be associated with hypoxia responses in tumors.

Furthermore, to investigate the LRRC59 modulating network, we investigated co-expression networks of LRRC59 in three microarray datasets of bladder cancer in GEO by using the SEEK platform (Fig. 6A). We found that the top-ranked co-expression genes were strongly correlated with cell cycle pathways and a couple of pathways involved in PTMs, including the regulation of protein modification and protein ubiquitination pathways in GO analyses (Fig. 6B and C; Supplementary Table S2).

Moreover, we performed PPI network analysis of LRRC59 using STRING and found that LRRC59 physically interacted complexes were predominantly located in the ER (Supplementary Fig. 4A and B). Functional enrichment analysis using Biological Process indicated that the function of LRRC59 networks was strongly correlated with fibroblast growth factor receptor signaling, which is an important hallmark in UC development (Supplementary Fig. 4C and D; Supplementary Fig. S5). The underlying mechanisms might be based on the interactions of fibroblast growth factor 1 (FGF1) with LRRC59 and KPN2A complexes in the nucleopore [18]. The roles of LRRC59 interaction networks in UC warrant further investigation.

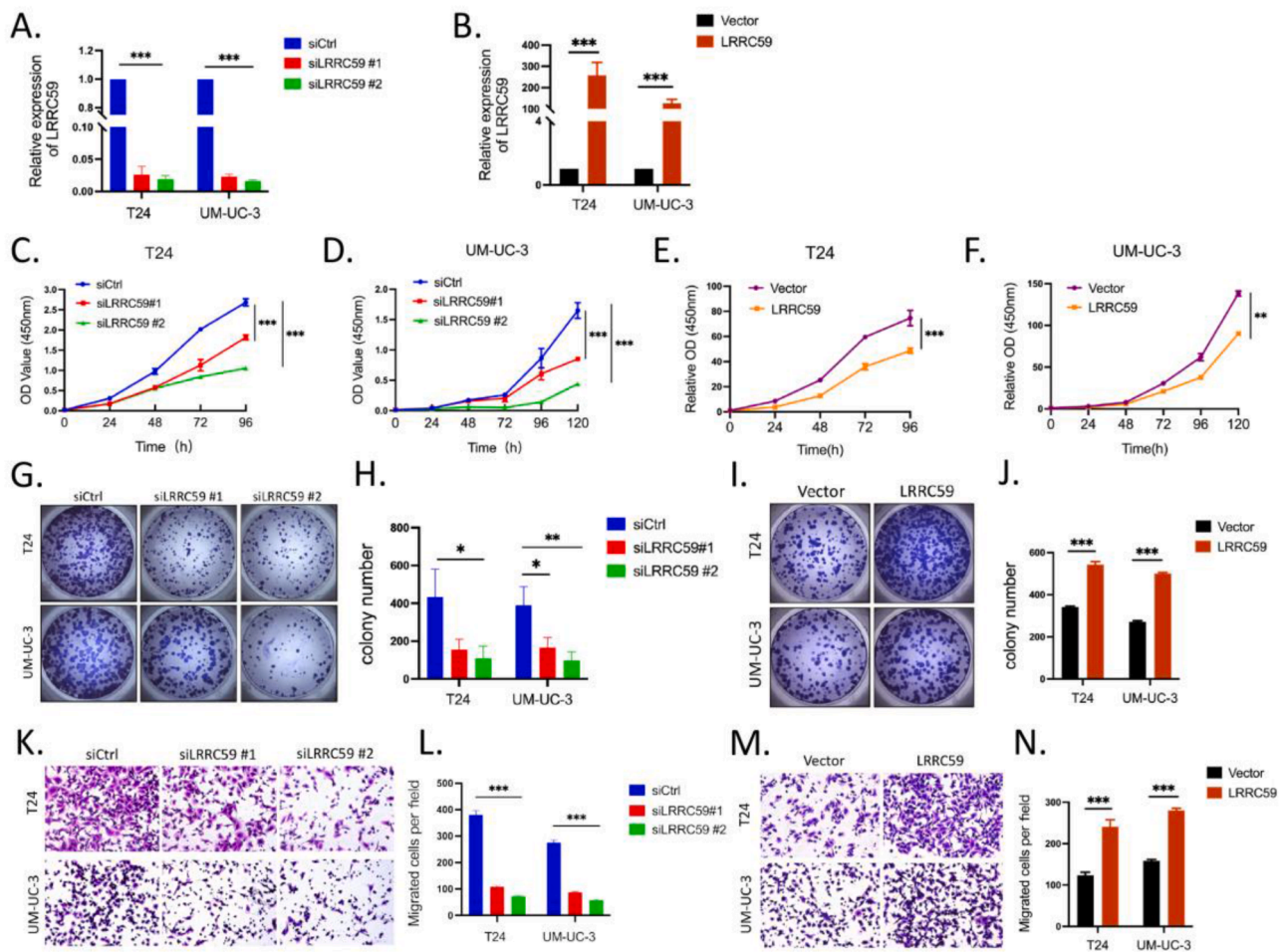


Fig. 5. LRRRC59 promoted the proliferation and migration of UC cells. (A, B) LRRRC59 was markedly downregulated or upregulated after siLRRRC59s or pcDNA3.1-LRRRC59 transfection. (C, D) SiRNA knockdown of LRRRC59 in T24 and UM-UC-3 cells significantly inhibited cell proliferation in CCK8 assay. (E, F) Overexpression of LRRRC59 in T24 and UM-UC-3 cells markedly increased cell proliferation in CCK8 assay. (G, H) Colony-formation assays demonstrated that LRRRC59 knockdown dramatically inhibited the size and number of colonies of T24 and UM-UC-3 cells. (I, J) The overexpression of LRRRC59 increased the size and number of colonies of T24 and UM-UC-3 cells. (K, L) The silencing of LRRRC59 reduced T24 and UM-UC-3 cell migration in the Transwell assay. (M, N) The expression of LRRRC59 increased T24 and UM-UC-3 cell migration in the Transwell assay. * $p < 0.05$; ** $p < 0.01$, *** $p < 0.001$.

Knockdown of LRRRC59 induced ER stress and dys-regulation of cell cycle genes in vitro

To further elucidate the oncogenic mechanisms of LRRRC59 in bladder cancer, we stimulated the bladder cancer cell line T24 and UM-UC-3 by using tunicamycin (TM), a chemical showing as a potent inducer of ER-stress in cells. We found that the stress-related marker HYOU1 and XBP1 were significantly enhanced by TM. Knockdown of LRRRC59 gene expression enhanced HYOU1 and XBP1-mediated ER-stress signaling (Fig. 7A and B). Meanwhile, E2F1, one of the important cell cycle-related transcriptional factors in bladder cancer was found decreased dramatically (Fig. 7C), consistent with our results in our FACS analysis of cell cycle arrest. Importantly, we found that knockdown of LRRRC59 significantly enhanced the sensitivity of Cisplatin to inhibit the viability of cell line UM-UC-3 (Fig. 7D and E). Our data suggests that LRRRC59 regulates the ER-stress signaling, regulates cell cycle, and modulates the treatment response of cisplatin in vitro. In-depth investigations on the molecular mechanisms of LRRRC59 in future may help to clarify LRRRC59 as a potential therapeutic target in bladder cancer.

Discussion

UC is a heterogeneous disease with high recurrence and mortality rates. Identifying novel prognostic biomarkers and establishing stable

predictive models are crucial in personalized medicine for patients with UC. In this study, we performed WSI analysis of IHC to investigate the expression pattern and clinical significance of LRRRC59 in 107 UC samples. We found that elevated expression of LRRRC59 was significantly correlated with poorer prognosis of UCs and consistently correlated with worse clinicopathological features, such as higher pathological grades and advanced stages. Moreover, our data showed that knockdown of LRRRC59 led to the inhibition of UC cell proliferation, migration, and induction of cell cycle arrest at the G1 phase, while overexpression of LRRRC59 promoted UC cell proliferation and migration. Mechanically, LRRRC59 regulates ER-stress signaling and cell cycle in UC cell lines. Our results suggest that LRRRC59 may serve as a novel prognostic factor in UC. Our results are consistent with the findings of previous studies on other cancers [14,19,20].

Previous studies showed that about one-third of patients with NMIBC have a lifelong risk of progression to MIBC or metastasis. The European Organization for Research and Treatment of Cancer risk table has been used for risk stratification and prognosis prediction in patients with NMIBC [21]. However, pathological features, molecular subtyping, and treatment approaches might have substantial influence on the classification of patients at high-risk. Therefore, patients with potentially worse outcomes remain likely to be misclassified, and the previously established subtyping systems are limited in clinical practice. LRRRC59 could serve as a potential biomarker to complement risk stratification and

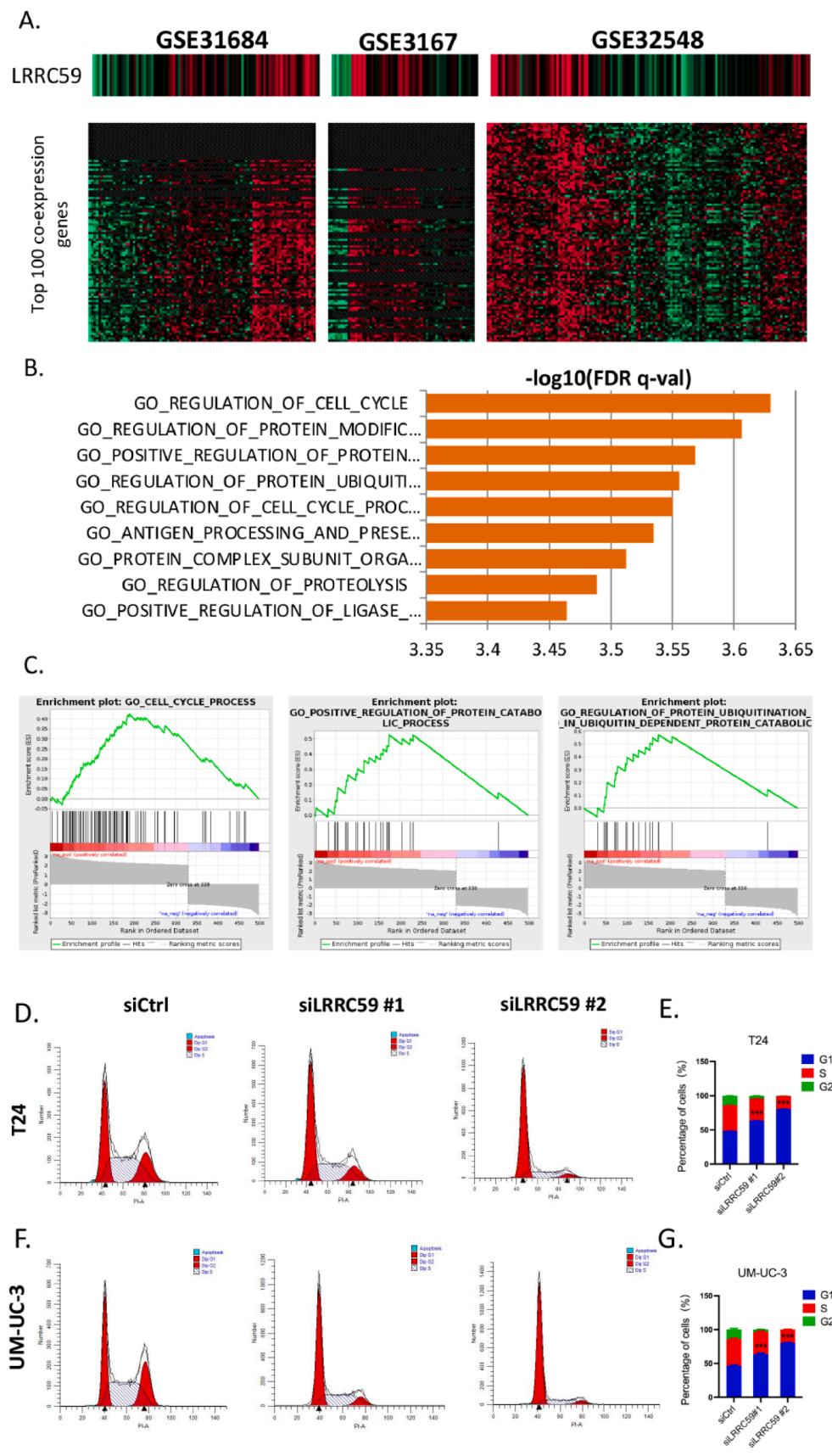


Fig. 6. Enrichment analysis of LRRC59 co-expressed genes in microarray datasets of bladder cancer and flow cytometry analysis of cell cycle. (A) The heatmap of the co-expression network of LRRC59 in bladder cancer microarray datasets. (B) Enrichment analysis of the co-expression genes of LRRC59. (C) Top-ranked enrichment plots in GSEA analysis for the LRRC59-positive correlation pathways. (D, E) The silencing of LRRC59 increased the percentage of G1 phase in T24 cells. (F, G) The silencing of LRRC59 increased the percentage of G1 phase in UM-UC-3 cells.

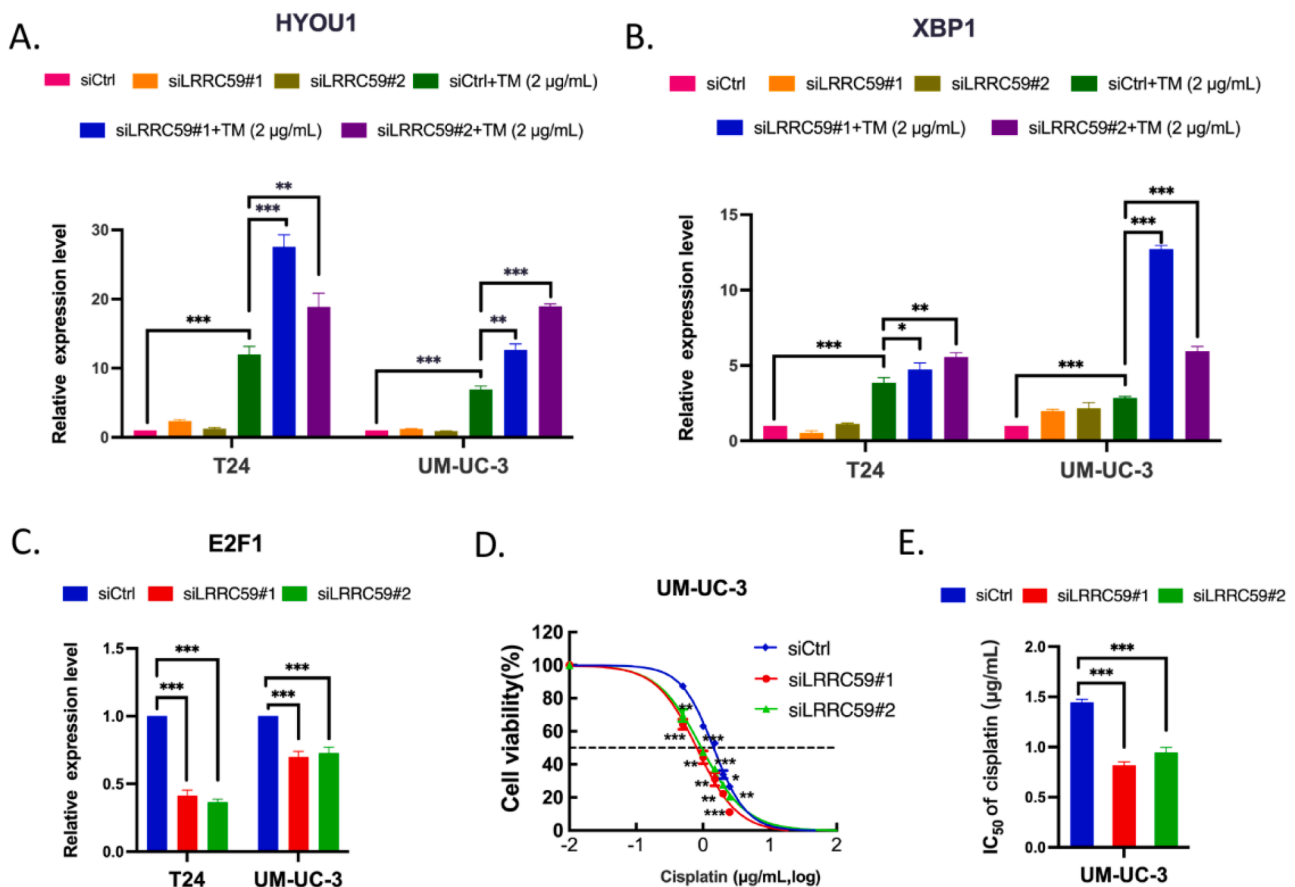


Fig. 7. Knockdown of LRRC59 induced ER stress and dys-regulation of cell cycle genes in vitro. (A) The expression of HYOU1 was upregulated after tunicamycin (TM) stimulation, and the expression of HYOU1 in both siLRRC59 and TM treatment was higher than TM treatment alone. (B) The expression of XBP1 was upregulated after tunicamycin (TM) stimulation, and the expression of XBP1 in both siLRRC59 and TM treatment was higher than TM treatment alone. (C) The expression of LRRC59 was down-regulated in T24 and UM-UC-3 cells after siLRRC59s transfection. (D, E) The IC₅₀ of cisplatin in LRRC59-downregulated UM-UC-3 cells was decreased compared to negative control. * $p < 0.05$; ** $p < 0.01$, *** $p < 0.001$.

identify patients with high-risk NMIBC for appropriate treatment.

Our analyses showed that the elevated expression of LRRC59 was significantly correlated with the prognosis of patients with bladder cancer in the TCGA-BLCA dataset. Moreover, the elevated expression of LRRC59 was also found significantly associated with the resistance to the treatment response in the TCGA-BLCA dataset (Supplementary Fig. S6A; Supplementary Table S3). Therefore, the evaluation of the expression levels of LRRC59 by using IHC assay may not only be useful in distinguishing high-risk patients with poor prognosis, but also be helpful in identification of patients with non-response to the treatment.

In addition to LRRC59, the expression levels of three members of the leucine-rich repeat-containing gene family were also found elevated in tumors compared to their normal counterparts in TCGA-BLCA dataset, including LRRC15, LRRC57, LRRC58 (Supplementary Fig. S6B–D). Among these, LRRC15 has been recently reported as a novel therapeutic target for multiple solid tumor indications [22–24]. The LRRC15⁺CAF (carcinoma-associated fibroblasts) subpopulation was found to be driven by TGF- β and correlated with a poor response to anti-PD-L1 therapy. Targeting LRRC15⁺CAF using combinatorial therapy approaches may improve immunotherapy responses in patients with cancer [25]. For LRRC59, it has been reported that LRRC59 is a regulator of DDX58, which is involved in type I IFN signaling that responds to viral infections [26]. In addition, LRRC59 participates in trafficking of NA-sensing TLRs from the ER and regulates TLR-mediated signaling [27]. These studies suggested that the members of the leucine-rich repeat-containing gene family such as LRRC15 and LRRC59 might play roles in the immune response.

In our data, we observed that elevated LRRC59 expression was significantly associated with a positive nodal status, but the underlying mechanisms underpinning lymph node (LN) metastasis remain unexplored. Recent studies have shown that stress-related RNA helicase protein Ddx21 [28], metabolic pathway regulatory factors YAP/TAZ [29], and specific immune environment in LN might facilitate tumor colonization and metastasis [30]. We found that LRRC59 is significantly correlated with multiple stress-related genes in TCGA-BLCA data including DDX21 (Supplementary Fig. S5D). Meanwhile, we validated that LRRC59 participates in the modulation of the ER-stress signaling mediated by HYOU1 and XBP1 (Fig. 7). Therefore, in future direction, investigation of relationships between the ER-stress and LN metastasis in UC might be helpful in elucidating the mechanisms underlying LN metastasis in UC.

LRRC59 is a tail-anchored protein with a single transmembrane domain close to its C-terminal end that localizes to the ER and nuclear envelope [31]. Recently, LRRC59 was recognized as a nuclear translocation of FGF1. FGF1 is known to potentially regulate tumor cell survival, migration, and invasion [18]. The upregulated expression of FGF1 could induce epithelial-mesenchymal transition, shorten the survival rate of patients with UC [32], and promote the metastatic capability of cancer cells [33–35]. Moreover, higher LRRC59 mRNA expression levels are correlate with worse clinical phenotypes in several cancer types, including lung adenocarcinoma [14], breast cancer [19], head and neck squamous cell carcinoma [20], and prostate cancer [34,36]. However, the role and biological function of LRRC59 in UC remain unclear.

LRRC59 knockdown by shRNA significantly suppressed cell

proliferation and metastasis in lung adenocarcinoma [14]. Consistently, our results showed that *in vitro* experiments by knocking down of LRRC59 led to inhibiting cell proliferation and migration. LRRC59 knockdown resulted in cell cycle arrest at the G1 phase. Kim et al. showed that LRRC59 and KPNB1 mediated cytoplasmic ketohexokinase-A to enter the nucleus, phosphorylate YWHAH, down-regulate CDH1, and facilitate the migration of breast cancer cells [37]. Previous studies demonstrated that LRRC59 could participate in regulating tumor cell motility and trigger cancer cell dissemination in triple-negative breast cancer [38]. Taken together, these studies suggest that LRRC59 may be a potential therapeutic target for cancer therapy in UC.

Mechanistically, the cytosolic part of LRRC59 facilitates its interaction with KPNs and transports FGF1 through nuclear pores into the nucleus in a Ran-dependent manner. Ectopic overexpression of FGF1 has been shown to be highly associated with cancer progression and prognosis in bladder cancer [39]. Recent studies have demonstrated that FGF inhibitors can be used to treat locally advanced/metastatic UC by targeting tumor-specific oncogenic signaling involving the tumor immune microenvironment [40]. Additionally, LRRC59 is necessary for the nuclear import of oncoprotein protein phosphatase 2A (PP2A, CIP2A) [41]. However, whether LRRC59 is involved in FGF1 or CIP2A function in the nucleus needs to be validated by further functional experiments.

The leucine-rich repeat (LRR) domain in LRRC59 may provide hits for its crucial functions in PTM processes [42]. Previous studies have shown that the LRR gene family plays an important role in cancers. For example, LRRC15 has been reported to contribute to cancer immunotherapy [25]. We found that LRRC59 was significantly associated with PSMDs (Supplementary Fig. S5B), a protein family comprising proteasome components. Such interactions imply that LRRC59 might also be involved in the ubiquitin proteasome system pathway, which is one of the most common PTMs of proteins. Mounting evidence suggests that aberrant ubiquitination may result in cancer development and progression [43]. Moreover, LRRC59 has been reported to interact directly with stress granule (SG) factors, including UBAP2L, PRRC2A, and PRRC2C [44,45]. Increasing evidence has shown that SGs play a crucial role in regulating cancer initiation, progression, metastasis, and therapeutic resistance [46,47]. The specific mechanisms of LRRC59 involvement in ubiquitination and SG formation need to be elucidated in future studies.

In summary, increased expression of LRRC59 was significantly correlated with worse clinical features of UC. Our study proved that LRRC59 could serve as an efficient predictive prognostic biomarker in UC. *In vitro* experiments revealed that LRRC59 regulates cell proliferation and metastasis. Our data highlight the crucial role of LRRC59-mediated PTM processes in UC development.

Data availability statement

The authors declare that data supporting the findings of this study are available within the article and its supplementary information files.

Funding

This work was supported by grants from National Natural Science Foundation of China (#81972731, #81773026) and Medical Scientific Research Foundation of Guangdong Province, China (A2015389).

Ethics approval and consent to participate

The study was approved by the Ethical Committee of the Second Affiliated Hospital and Yuying Children's Hospital of WMU (2021-K-101-01). Written informed consent was obtained from all patients.

CRedit authorship contribution statement

Lu Pei: Validation, Writing – original draft, Visualization. **Qingfeng Zhu:** Investigation. **Xiaoping Zhuang:** Formal analysis. **Honglian Ruan:** Software, Formal analysis. **Zhiguang Zhao:** Formal analysis. **Haide Qin:** Conceptualization, Supervision, Methodology, Software, Formal analysis, Writing – review & editing. **Qiongqiong Lin:** Data curation, Writing – original draft.

Declaration of Competing Interest

The authors declare that the research was conducted in the absence of any commercial or financial relationships that could be construed as a potential conflict of interest.

Supplementary materials

Supplementary material associated with this article can be found, in the online version, at [doi:10.1016/j.tranon.2022.101474](https://doi.org/10.1016/j.tranon.2022.101474).

References

- [1] O. Sanli, J. Dobruch, M.A. Knowles, M. Burger, M. Alemozaffar, M.E. Nielsen, et al., Bladder cancer, *Nat. Rev. Dis. Prim.* 3 (2017) 17022, <https://doi.org/10.1038/nrdp.2017.22>.
- [2] J.A. Witjes, H.M. Bruins, R. Cathomas, E.M. Comperat, N.C. Cowan, G. Gakis, et al., European association of urology guidelines on muscle-invasive and metastatic bladder cancer: summary of the 2020 guidelines, *Eur. Urol.* 79 (1) (2021) 82–104, <https://doi.org/10.1016/j.eururo.2020.03.055>. Epub 2020/05/04.
- [3] M.J. Shi, X.Y. Meng, Q.J. Wu, X.H. Zhou, High CD3D/CD4 ratio predicts better survival in muscle-invasive bladder cancer, *Cancer Manag. Res.* 11 (2019) 2987–2995, <https://doi.org/10.2147/CMAR.S191105>. Epub 2019/05/23.
- [4] M. Huang, W. Dong, R. Xie, J. Wu, Q. Su, W. Li, et al., HSF1 facilitates the multistep process of lymphatic metastasis in bladder cancer via a novel Prmt5-Wdr5-dependent transcriptional program, *Cancer Commun.* 42 (5) (2022) 447–470, <https://doi.org/10.1002/cac2.12284> (*Lond*)Epub 2022/04/19.
- [5] L.A. Kluth, E. Xylinas, M. Rieken, M. Kent, M. Ikeda, K. Matsumoto, et al., Prognostic model for predicting survival in patients with disease recurrence following radical cystectomy, *Eur. Urol. Focus* 1 (1) (2015) 75–81, <https://doi.org/10.1016/j.euf.2014.10.003>. Epub 2015/08/01.
- [6] S.X. Wu, J. Huang, Z.W. Liu, H.G. Chen, P. Guo, Q.Q. Cai, et al., A genomic-clinicopathologic nomogram for the preoperative prediction of lymph node metastasis in bladder cancer, *EBioMedicine* 31 (2018) 54–65, <https://doi.org/10.1016/j.ebiom.2018.03.034>.
- [7] W. Choi, S. Porten, S. Kim, D. Willis, E.R. Plimack, J. Hoffman-Censits, et al., Identification of distinct basal and luminal subtypes of muscle-invasive bladder cancer with different sensitivities to frontline chemotherapy, *Cancer Cell* 25 (2) (2014) 152–165, <https://doi.org/10.1016/j.ccr.2014.01.009>.
- [8] M. Babjuk, M. Burger, O. Capoun, D. Cohen, E.M. Compérat, J.L. Dominguez Escrig, et al., European Association of urology guidelines on non-muscle-invasive bladder cancer (Ta, T1, and carcinoma *in situ*), *Eur. Urol.* 81 (1) (2022) 75–94, <https://doi.org/10.1016/j.eururo.2021.08.010>.
- [9] E. Madden, S.E. Logue, S.J. Healy, S. Manie, A. Samali, The role of the unfolded protein response in cancer progression: from oncogenesis to chemoresistance, *Biol. Cell.* 111 (1) (2019) 1–17, <https://doi.org/10.1111/boc.201800050>. Epub 2018/10/12.
- [10] L. Sisinni, M. Pietrafesa, S. Lepore, F. Maddalena, V. Condelli, F. Esposito, et al., Endoplasmic reticulum stress and unfolded protein response in breast cancer: the balance between apoptosis and autophagy and its role in drug resistance, *Int. J. Mol. Sci.* 20 (4) (2019), <https://doi.org/10.3390/ijms20040857>. Epub 2019/02/20.
- [11] M. Wang, R.J. Kaufman, The impact of the endoplasmic reticulum protein-folding environment on cancer development, *Nat. Rev. Cancer* 14 (9) (2014) 581–597, <https://doi.org/10.1038/nrc3800>. Epub 2014/08/26.
- [12] C.H. Wu, C.R. Silvers, E.M. Messing, Y.F. Lee, Bladder cancer extracellular vesicles drive tumorigenesis by inducing the unfolded protein response in endoplasmic reticulum of nonmalignant cells, *J. Biol. Chem.* 294 (9) (2019) 3207–3218, <https://doi.org/10.1074/jbc.RA118.006682>. Epub 2018/12/30.
- [13] M.B. Amin, F.L. Greene, et al., *AJCC Cancer Staging Manual, 8th*, Springer, New York, 2017.
- [14] D. Li, Y. Xing, T. Tian, Y. Guo, J. Qian, Overexpression of LRRC59 is associated with poor prognosis and promotes cell proliferation and invasion in lung adenocarcinoma, *Onco Targets Ther.* 13 (2020) 6453–6463, <https://doi.org/10.2147/OTT.S245336>. Epub 2020/08/06.
- [15] D. Liu, G. Sharbeen, P. Phillips, Australian pancreatic cancer genome I, Ford CE, ROR1 and ROR2 expression in pancreatic cancer, *BMC Cancer* 21 (1) (2021) 1199, <https://doi.org/10.1186/s12885-021-08952-9>. Epub 2021/11/13.
- [16] P. Bankhead, M.B. Loughrey, J.A. Fernández, Y. Dombrowski, D.G. McArt, P. D. Dunne, et al., QuPath: open source software for digital pathology image

- analysis, *Sci. Rep.* 7 (1) (2017) 16878, <https://doi.org/10.1038/s41598-017-17204-5>.
- [17] F. Zeng, L. Luo, D. Li, J. Guo, M. Guo, KPN2 interaction with CBX8 contributes to the development and progression of bladder cancer by mediating the PRDM1/C-FOS pathway, *J. Transl. Med.* 19 (1) (2021) 112, <https://doi.org/10.1186/s12967-021-02709-5>. Epub 2021/03/19.
- [18] Y. Zhen, V. Sorensen, C.S. Skjerpren, E.M. Haugsten, Y. Jin, S. Walchli, et al., Nuclear import of exogenous FG1 requires the Er-protein LRRC59 and the importins Kpnalpha1 and Kpnbeta1, *Traffic* 13 (5) (2012) 650–664, <https://doi.org/10.1111/j.1600-0854.2012.01341.x>. Epub 2012/02/11.
- [19] H. Toda, S. Kurozumi, Y. Kijima, T. Idichi, Y. Shinden, Y. Yamada, et al., Molecular pathogenesis of triple-negative breast cancer based on microRNA expression signatures: antitumor miR-204-5p targets AP1S3, *J. Hum. Genet.* 63 (12) (2018) 1197–1210, <https://doi.org/10.1038/s10038-018-0510-3>. Epub 2018/09/20.
- [20] X. Geng, Y. Zhang, Z. Zeng, Z. Zhu, H. Wang, W. Yu, et al., Molecular characteristics, prognostic value, and immune characteristics of M(6)a regulators identified in head and neck squamous cell carcinoma, *Front. Oncol.* 11 (2021), 629718, <https://doi.org/10.3389/fonc.2021.629718>. Epub 2021/04/06.
- [21] V. Soukup, O. Capoun, D. Cohen, V. Hernandez, M. Burger, E. Comperat, et al., Risk stratification tools and prognostic models in non-muscle-invasive bladder cancer: a critical assessment from the European association of urology non-muscle-invasive bladder cancer guidelines panel, *Eur. Urol. Focus* 6 (3) (2020) 479–489, <https://doi.org/10.1016/j.euf.2018.11.005>. Epub 2018/11/25.
- [22] J.W. Purcell, S.G. Tanlimco, J. Hickson, M. Fox, M. Sho, L. Durkin, et al., LRRC15 is a novel mesenchymal protein and stromal target for antibody-drug conjugates, *Cancer Res.* 78 (14) (2018) 4059–4072, <https://doi.org/10.1158/0008-5472.CAN-18-0327>. Epub 2018/05/17.
- [23] U. Ray, D.B. Jung, L. Jin, Y. Xiao, S. Dasari, S. Sarkar Bhattacharya, et al., Targeting LRRC15 inhibits metastatic dissemination of ovarian cancer, *Cancer Res.* 82 (6) (2022) 1038–1054, <https://doi.org/10.1158/0008-5472.CAN-21-0622>. Epub 2021/10/17.
- [24] U. Ray, C.L. Pathoulas, P. Thirusangu, J.W. Purcell, N. Kannan, V. Shridhar, Exploiting LRRC15 as a novel therapeutic target in cancer, *Cancer Res.* 82 (9) (2022) 1675–1681, <https://doi.org/10.1158/0008-5472.CAN-21-3734>. Epub 2022/03/10.
- [25] C.X. Dominguez, S. Muller, S. Keerthivasan, H. Koeppen, J. Hung, S. Gierke, et al., Single-cell RNA sequencing reveals stromal evolution into LRRC15(+) myofibroblasts as a determinant of patient response to cancer immunotherapy, *Cancer Discov.* 10 (2) (2020) 232–253, <https://doi.org/10.1158/2159-8290.CD-19-0644>. Epub 2019/11/09.
- [26] H. Xian, S. Yang, S. Jin, Y. Zhang, J. Cui, LRRC59 modulates type I interferon signaling by restraining the SQSTM1/P62-mediated autophagic degradation of pattern recognition receptor DDX58/RIG-I, *Autophagy* 16 (3) (2020) 408–418, <https://doi.org/10.1080/15548627.2019.1615303>. Epub 2019/05/10.
- [27] M. Tatematsu, K. Funami, N. Ishii, T. Seya, C. Obuse, M. Matsumoto, LRRC59 regulates trafficking of nucleic acid-sensing TLRs from the endoplasmic reticulum via association with UNC93B1, *J. Immunol.* 195 (10) (2015) 4933–4942, <https://doi.org/10.4049/jimmunol.1501305>. Epub 2015/10/16.
- [28] K. Koltowska, K.S. Okuda, M. Gloger, M. Rondon-Galeano, E. Mason, J. Xuan, et al., The RNA helicase DDX21 controls Vegf-driven developmental lymphangiogenesis by balancing endothelial cell ribosome biogenesis and P53 function, *Nat. Cell Biol.* 23 (11) (2021) 1136–1147, <https://doi.org/10.1038/s41556-021-00784-w>. Epub 2021/11/10.
- [29] J.M. Ubellacker, S.J. Morrison, Metabolic adaptation fuels lymph node metastasis, *Cell Metab.* 29 (4) (2019) 785–786, <https://doi.org/10.1016/j.cmet.2019.03.006>. Epub 2019/04/04.
- [30] N.E. Reticker-Flynn, W. Zhang, J.A. Belk, P.A. Basto, N.K. Escalante, G.O. W. Pilarowski, et al., Lymph node colonization induces tumor-immune tolerance to promote distant metastasis, *Cell* 185 (11) (2022) 1924–1942, <https://doi.org/10.1016/j.cell.2022.04.019>, e23. Epub 2022/05/08.
- [31] M. Blenski, R.H. Kehlenbach, Targeting of LRRC59 to the endoplasmic reticulum and the inner nuclear membrane, *Int. J. Mol. Sci.* 20 (2) (2019), <https://doi.org/10.3390/ijms20020334>. Epub 2019/01/18.
- [32] J. Wang, M. Guo, X. Zhou, Z. Ding, X. Chen, Y. Jiao, et al., Angiogenesis related gene expression significantly associated with the prognostic role of an urothelial bladder carcinoma, *Transl. Androl. Urol.* 9 (5) (2020) 2200–2210, <https://doi.org/10.21037/tau-20-1291>. Epub 2020/11/20.
- [33] M.G. Terp, R.R. Lund, O.N. Jensen, R. Leth-Larsen, H.J. Ditzel, Identification of markers associated with highly aggressive metastatic phenotypes using quantitative comparative proteomics, *Cancer Genom. Proteom.* 9 (5) (2012) 265–273. Epub 2012/09/20.
- [34] Y.P. Yu, P. Liu, J. Nelson, R.L. Hamilton, R. Bhargava, G. Michalopoulos, et al., Identification of Recurrent fusion genes across multiple cancer types, *Sci. Rep.* 9 (1) (2019) 1074, <https://doi.org/10.1038/s41598-019-38550-6>. Epub 2019/02/02.
- [35] Z. Tang, B. Kang, C. Li, T. Chen, Z. Zhang, GEPIA2: an enhanced web server for large-scale expression profiling and interactive analysis, *Nucleic Acids. Res.* 47 (W1) (2019) W556–W560, <https://doi.org/10.1093/nar/gkz430>. Epub 2019/05/23.
- [36] Y.P. Yu, S. Liu, J. Nelson, J.H. Luo, Detection of fusion gene transcripts in the blood samples of prostate cancer patients, *Sci. Rep.* 11 (1) (2021) 16995, <https://doi.org/10.1038/s41598-021-96528-9>. Epub 2021/08/22.
- [37] J. Kim, J. Kang, Y.L. Kang, J. Woo, Y. Kim, J. Huh, et al., Ketohehexokinase-A acts as a nuclear protein kinase that mediates fructose-induced metastasis in breast cancer, *Nat. Commun.* 11 (1) (2020) 5436, <https://doi.org/10.1038/s41467-020-19263-1>. Epub 2020/10/30.
- [38] E. Maurizio, J.R. Wisniewski, Y. Ciani, A. Amato, L. Arnoldo, C. Penzo, et al., Translating proteomic into functional data: an high mobility group A1 (HMGAI1) proteomic signature has prognostic value in breast cancer, *Mol. Cell. Proteom.* 15 (1) (2016) 109–123, <https://doi.org/10.1074/mcp.M115.050401>. Epub 2015/11/04.
- [39] N. Liu, J. Zhang, S. Sun, L. Yang, Z. Zhou, Q. Sun, et al., Expression and clinical significance of fibroblast growth factor 1 in gastric adenocarcinoma, *Oncotargets Ther.* 8 (2015) 615–621, <https://doi.org/10.2147/OTT.S79204>. Epub 2015/03/21.
- [40] H.W. Lee, H.K. Seo, Fibroblast growth factor inhibitors for treating locally advanced/metastatic bladder urothelial carcinomas via dual targeting of tumor-specific oncogenic signaling and the tumor immune microenvironment, *Int. J. Mol. Sci.* 22 (17) (2021), <https://doi.org/10.3390/ijms22179526>. Epub 2021/09/11.
- [41] R. Pallai, A. Bhaskar, N. Barnett-Bernodat, C. Gallo-Ebert, M. Pusey, J.T. Nickels, et al., Leucine-rich repeat-containing protein 59 mediates nuclear import of cancerous inhibitor of Pp2a in prostate cancer cells, *Tumour Biol.* 36 (8) (2015) 6383–6390, <https://doi.org/10.1007/s13277-015-3326-1>. Epub 2015/04/03.
- [42] Y. Du, T. Duan, Y. Feng, Q. Liu, M. Lin, J. Cui, et al., Lrrc25 inhibits type I IFN signaling by targeting Isg15-associated Rig-I for autophagic degradation, *EMBO J.* 37 (3) (2018) 351–366, <https://doi.org/10.15252/embj.201796781>. Epub 2017/12/31.
- [43] L. Deng, T. Meng, L. Chen, W. Wei, P. Wang, The role of ubiquitination in tumorigenesis and targeted drug discovery, *Sign. Transduct. Target Ther.* 5 (1) (2020) 11, <https://doi.org/10.1038/s41392-020-0107-0>. Epub 2020/04/17.
- [44] M.M. Hannigan, A.M. Hoffman, J.W. Thompson, T. Zheng, C.V. Nicchitta, Quantitative proteomics links the LRRC59 interactome to mRNA translation on the ER membrane, *Mol. Cell. Proteom.* 19 (11) (2020) 1826–1849, <https://doi.org/10.1074/mcp.RA120.002228>. Epub 2020/08/14.
- [45] J.Y. Youn, W.H. Dunham, S.J. Hong, J.D.R. Knight, M. Bashkurov, G.I. Chen, et al., High-density proximity mapping reveals the subcellular organization of MRNA-associated granules and bodies, *Mol. Cell* 69 (3) (2018) 517–532, <https://doi.org/10.1016/j.molcel.2017.12.020>, e11. Epub 2018/02/06.
- [46] S.P. Somasekharan, A. El-Naggar, G. Leprivier, H. Cheng, S. Hajee, T.G. Grunewald, et al., Yb-1 regulates stress granule formation and tumor progression by translationally activating G3bp1, *J. Cell Biol.* 208 (7) (2015) 913–929, <https://doi.org/10.1083/jcb.201411047>. Epub 2015/03/25.
- [47] Q. Shi, Y. Zhu, J. Ma, K. Chang, D. Ding, Y. Bai, et al., Prostate cancer-associated SPOP mutations enhance cancer cell survival and docetaxel resistance by upregulating caprin1-dependent stress granule assembly, *Mol. Cancer* 18 (1) (2019) 170, <https://doi.org/10.1186/s12943-019-1096-x>. Epub 2019/11/28.